Journal Of Natural Products
July 2020, Volume 83 Issue 7 Pages 2299-2304
https://doi.org/10.1021/acs.jnatprod.0c00223
https://archimer.ifremer.fr/doc/00695/80730/

Futunamine, a Pyrrole-Imidazole Alkaloid from the Sponge *Stylissa* aff. *carteri* Collected off the Futuna Islands

Miguel-Gordo Maria [2, 3], Gegunde Sandra [1], Jennings Laurence K. [2, 3], Genta-Jouve Gregory [4, 5], Calabro Kevin [2, 3], Alfonso Amparo [1], Botana Luis M. [1, *], Thomas Olivier P. [2, 3, *]

[1] Univ Santiago de Compostela, Fac Vet, Dept Farmacol, Lugo 27002, Spain.
[2] Natl Univ Ireland Galway NUI Galway, Sch Chem, Marine Biodiscovery, Galway H91 TK33, Ireland.
[3] Natl Univ Ireland Galway NUI Galway, Ryan Inst, Galway H91 TK33, Ireland.
[4] Univ Paris 05, Lab Chim Toxicol Analyt & Cellulaire C TAC, UMR CNRS CiTCoM 8038, F-75006 Paris, France.
[5] Univ Guyane, Lab Ecol Evolut Interact Syst Amazoniens LEEISA, USR 3456, Cayenne 97334, French Guiana.

* Corresponding authors : Luis M. Botana, email address : luis.botana@usc.es ; Olivier P. Thomas, email address : olivier.thomas@nuigalway.ie

Abstract :

The chemical investigation of the sponge Stylissa aff. carteri collected around Futuna Islands in the Pacific Ocean led to the isolation of three new dimeric pyrrole 2-aminoimidazole alkaloids (PIAs). Futunamine (1) features an unprecedented pyrrolo[1,2-c]imidazole core, while two other new dimeric PIAs were identified as analogues of palau'amine. Together with other known PIAs isolated from this species, they were shown to exhibit antiinflammatory and neuroprotective activities.

Graphical abstract

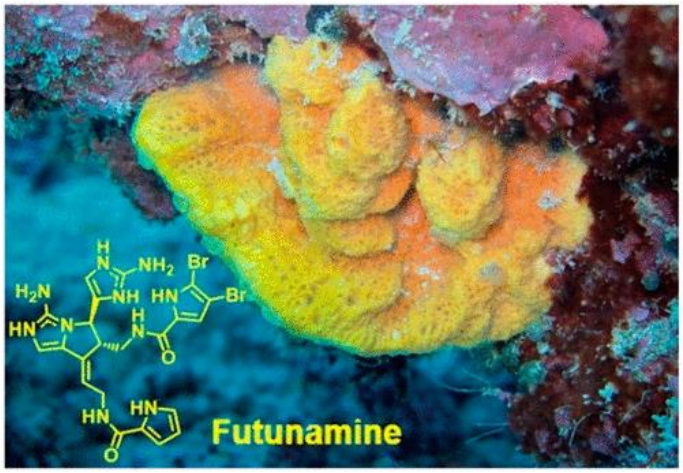

Pyrrole-imidazole alkaloids (PIAs) constitute a well-known family of sponge natural products.[1] Since the isolation of the first member of this structural class in 1969, dibromophakellin from the sponge *Phakellia flabellata*, over 220 different PIAs have been identified.[2] Oroidin was isolated in 1971 from the sponge *Agelas oroides*, and it is considered a key biogenetic precursor to most metabolites of the PIA family. Most PIAs have been isolated from sponges belonging to genera *Agelas, Phakellia*, *Axinella*, *Hymeniacidon* and *Stylissa*. This family of marine natural products is continuously expanding. It has attracted the attention of organic chemists due to PIAs potent biological activities and fascinating architectures representing challenges for total syntheses.

A first inventory of sponges around the Futuna Islands in the Tropical Southwestern Pacific was performed as part of the *Tara* Pacific expedition.[3] After preliminary chemical and biological screenings on fractions prepared from the collected invertebrates, the sponge *Stylissa* aff. *carteri* (Dendy, 1889) was selected for chemical investigation. The UHPLC-HRMS dereplication of *Stylissa* aff. *carteri* fractions from its MeOH extract using the database MarinLit revealed unknown brominated compounds belonging to the PIA family. Previous chemical studies on the sponge *Axinella* (aka *Stylissa*) *carteri* led to the identification of cyclopeptides,[4] stylissazoles A-C,[5] carteramine A,[6] and ageliferin and other PIAs.[7]

Herein is described the first chemical study on the shallow-water sponge *Stylissa* aff. *carteri* commonly found around Futuna Islands. Isolation and identification of three new dimeric PIAs are reported: futunamine (**1**) featuring a new pyrrolo[1,2-*c*]imidazole core, two new hexacyclic analogues of palau'amine and styloguanidine named debromokonbu'acidin (**2**) and didebromocarteramine (**3**) respectively; together with the

known sceptrin,[8] manzacidin A (**4**),[7] hymenidin (**5**),[9] and oroidin (**6**).[10] These compounds were tested for their anti-inflammatory and neuroprotective activities on human neuroblastoma SH-SY5Y and microglia BV2 cells.

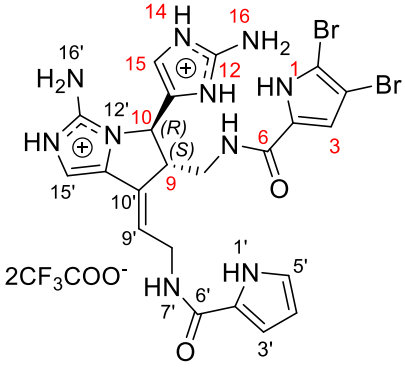

Futunamine (**1**)

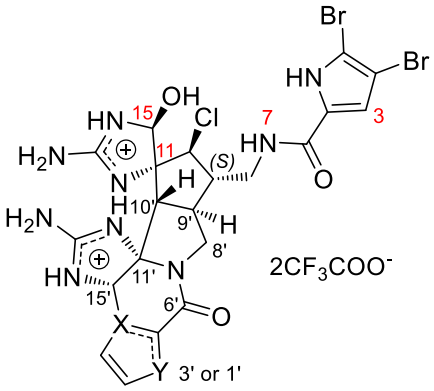

	X	Y
Debromokonbu'acidin (**2**)	N	CH
Didebromocarteramine (**3**)	C	NH

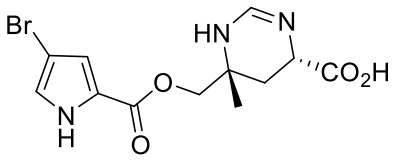

Manzacidin A (**4**)

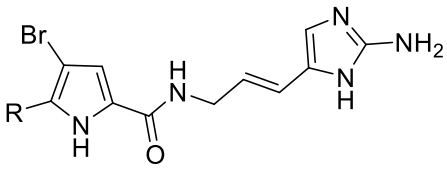

	R
Hymenidin (**5**)	H
Oroidin (**6**)	Br

Compound **1** was isolated as a yellow amorphous solid and the (+)-HRESIMS spectrum displayed a protonated molecule $[M+H]^+$ at *m/z* 617.0382 with a 1:2:1 isotopic splitting pattern, characteristic of the presence of two bromine atoms, leading to the molecular formula $C_{22}H_{22}Br_2N_{10}O_2$, with 16 indices of hydrogen deficiency. NMR data recorded in CD_3OD revealed seven signals corresponding to olefinic/aromatic protons, three of them being identified as aromatic protons of a 2-acylsubstituted pyrrole at δ_H 6.84 (dd, J = 3.5, 1.0 Hz, H-3'), 6.21 (dd, J = 3.5, 2.5 Hz, H-4') and 6.97 (dd, J = 2.5, 1.0 Hz, H-5') (Table 1). An additional signal of an aromatic hydrogen was assigned to a 2-acyl-4,5-dibromosubstituted pyrrole proton with a characteristic chemical shift at δ_H 6.74 (s, H-3).

This hydrogen showed HMBC correlations with C-2, C-4 and C-5 (Figure 1). Another two signals were assigned to methines of two 2-aminoimidazole rings at δ_H 6.79 (s, H-15') and 6.57 (br s, H-15). Analysis of the HMBC spectrum showed correlations of H-15' and H-15 correlated with signals of two guanidine carbons at δ_C 147.3 (C-13') and 149.5 (C-13), respectively. Altogether, these first conclusions supported the dimeric nature of **1**. Analysis of 1D and 2D NMR data indicated an ABX spin system consisting of a methylene with resonances at δ_H 3.74 (dd, J = 14.0, 4.0 Hz, H-8a) and 3.46 (dd, J = 14.0, 7.0 Hz, H-8b) coupled with a methine at δ_H 3.05 (dd, J = 7.0, 4.0 Hz, H-9) which was further connected with a methine at δ_H 5.57 (br s, H-10) and δ_C 48.8 (C-10). Analysis of the HMBC spectrum showed that H-10 was connected to an imidazole ring through a key H-10/C-15 HMBC correlation. A second spin system was constituted by methylene signals at δ_H 4.12 (d, J = 17 Hz, H-8'a) and 4.08 (d, J = 17.0 Hz, H-8'b) vicinal to an olefin hydrogen at δ_H 6.52 (br s, H-9') and δ_C 113.0 (C-9'). Key H-8'/C-10', H-9'/C-11' and H-15'/C-11' HMBC correlations allowed the construction of the fragment from CH-9' to C-15'. The C-9/C-10' connection was established by analysis of HMBC correlations from H-8, H-9 and H-10 to C-10', and from H-9 to C-9'. The C-10/NH-12 attachment was evidenced from HMBC correlations observed between H-10 and C-13' and C-11', revealing the pyrrolo[1,2-*c*]imidazole core moiety.

Table 1. NMR data for compound **1** in MeOH-d_4 (^{1}H 500 MHz and ^{13}C 125 MHz) and in DMSO-d_6 (^{1}H 600 MHz and ^{13}C 150 MHz).

	1			
	MeOH-d_4		DMSO-d_6	
Position	δ_C, type	δ_H, mult. (*J* in Hz)	δ_C, type	δ_H, mult. (*J* in Hz)
1 NH	-	-	-	12.75, br s
2	128.0, C	-	125.3, C	-
3	114.2, CH	6.75, s	112.9, CH	6.89, s
4	97.4, C	-	97.9, C	-
5	106.4, C	-	105.0, C	-
6	161.9, C	-	159.4, C	-
7 NH	-	-	-	8.40, t (6.0)
8a	40.8, CH_2	3.74, dd (14.0, 4.0)	39.5[a], CH_2	3.41[b]
8b		3.46, dd (14.0, 7.0)		3.28[b]
9	44.1, CH	3.05, dd (7.0, 4.0)	42.1, CH	2.97, dd (7.5, 5.0)
10	48.8, CH	5.57, s	46.4, CH	5.44, br s
11	124.3, C	-	123.1, C	-
12 NH	-	-	-	12.05, br s
13	149.5, C	-	147.7, C	-
14 NH	-	-	-	12.17, br s
15	112.0, CH	6.57, s	111.1, CH	6.64, br s
16 NH_2	-	-	-	7.51, br s
1' NH	-	-	-	11.57, s
2'	125.9, C	-	127.8, C	-
3'	112.1, CH	6.84, dd (3.5, 1.0)	110.8, CH	6.88, m
4'	110.4, CH	6.21, dd (3.5, 2.5)	109.0, CH	6.13, dt (3.5, 2.5)
5'	123.4, CH	6.97, dd (2.5, 1.0)	122.1, CH	6.95, m
6'	164.2, C	-	161.4, C	-
7' NH	-	-	-	8.71, br s
8'a	43.8, CH_2	4.12, d (17.0)	42.5, CH_2	4.02, d (4.5)
8'b		4.08, d (17.0)		
9'	113.0, CH	6.52, br s	110.7, CH	6.34, br s
10'	134.7, C	-	134.1, C	-
11'	123.3, C	-	121.2, C	-
13'	147.3, C	-	145.8, C	-
14' NH	-	-	-	12.32, br s
15'	110.0, CH	6.79, s	109.2, CH	6.96, s
16' NH_2	-	-	-	8.01, br s

[a] Overlapped with signals of the solvent, [b] overlapped with HOD

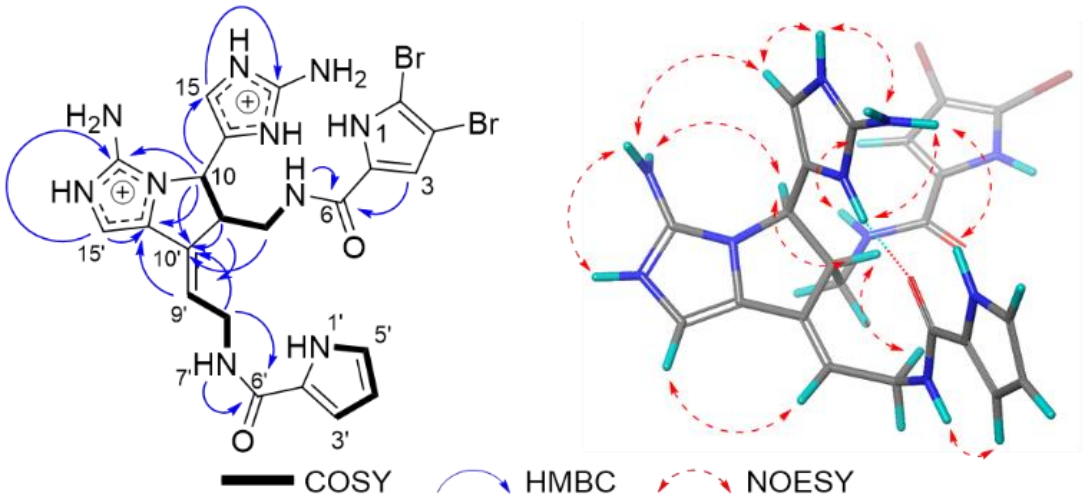

Figure 1. Key COSY, HMBC and NOESY NMR correlations of **1** in DMSO-d_6

Even though the core of the molecule was elucidated, some uncertainties remained, especially the location of the brominated pyrrole ring, and some relays through NH-7 and NH-7' were required to complete the planar structure of **1**. A second set of NMR data recorded in DMSO-d_6 aimed to position the brominated pyrrole ring and to confirm the planar structure of **1**. A key H-3/NH-7 nOe that unequivocally placed the dibrominated pyrrole ring attached to CH_2-8, while a H-3'/NH-7' nOe confirmed the location of the non-brominated pyrrole connected to CH_2-8. The NOESY spectrum also allowed the assignment of olefin geometry by observing H-15'/H-9' and H-9/H-8' nOe, consistent with an *E* configuration. The determination of the relative configuration between the two chiral centers C-9 and C-10 was not straightforward, since nOes and coupling constant values can be misleading for a five-membered ring. Additionally, many nOe correlations indicated a high flexibility and rotation within **1**. Since the calculation of total nuclear spin-spin coupling (Hz) has successfully been applied for the assignment of relative configurations around five-membered rings, we first performed a conformational analysis and *J*-coupling calculation on the pyrrolo[1,2-*c*]imidazole core. We could estimate theoretical $^3J_{H9\text{-}H10}$ value of 0.5 Hz for the *trans* and 6.7 Hz for the *cis* relative configurations (Figure S6). Since the vicinal coupling between

H-9 and H-10 was ~ 0 Hz in the ^{1}H NMR spectra obtained in MeOH-d_4 and in DMSO-d_6, a *trans* relative configuration was assigned for these hydrogens. The NH-1'/NH2-16 nOe correlation supported the assumption of a correct conformation for the theoretical calculation and ultimately for the relative configuration. The absolute configuration of **1** was deduced by comparison between experimental and theoretical electronic circular dichroism (ECD) analyses, with *E*, 9*S*, 10*R* assignments.

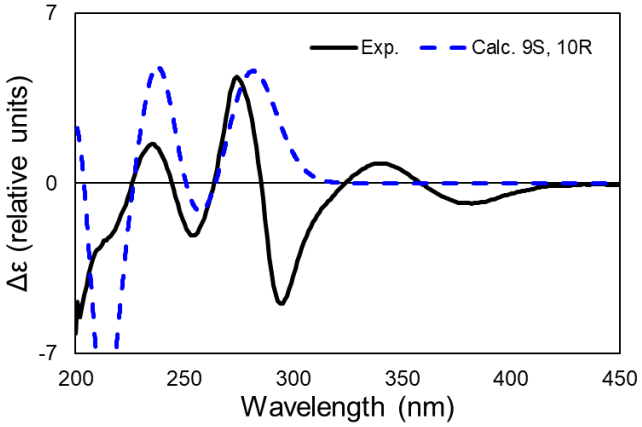

Figure 2. Comparison of the experimental and calculated ECD spectra of **1**.

Compound **2** was isolated as a yellow amorphous solid. Its molecular formula $C_{22}H_{23}Br_2ClN_{10}O_3$ was deduced from the $[M+H]^+$ ion at *m/z* 669.0092, with a 2:4:3:1 isotopic pattern, characteristic of one chlorine and two bromine atoms in the structure. Analysis of the MS/MS spectrum suggested the loss of a hydroxy (-18 amu) and of a non-brominated fragment at *m/z* 420.1664 (-251 amu), corresponding to a 4,5-dibromopyrrole carbonyl moiety. The presence of a chlorine atom in the molecule suggested a structure relationship with palau'amine or styloguanidine alkaloids, while the 4,5-dibromopyrrole carbonyl group was indicative of carteramine A[6] or konbu'acidin A[11] types of PIA. Confirmation of the chlorinated azabicyclo[3.3.0]octane central moiety was deduced from the key H-8'/H-9'/H-10'/H-9/H-10 COSY correlations, as well by the characteristic spiro carbon at δ_C 70.2 (qC, C-11). The spin system including hydrogens with signals

at δ_H 6.72 (dd, H-3'), 6.33 (br t, H-4') and 7.16 (br t, H-5') was indicative of a 1,2-disubstituted pyrrole. Therefore compound **2** corresponded to a debrominated konbu'acidin analogue.[11] The relative configuration of **2** was as the same as for palau'amine and konbu'acidin B since ^{1}H and ^{13}C NMR signals were very similar for these compounds (NMR data of **2** in Table S5). Since the ECD spectrum of **2** exhibited the same positive Cotton effect at 275 nm, with a shoulder at 248 nm, as observed for palau'amine, for which the relative and absolute configuration have been previously established, [12] compound **2** was assumed to have the same 15'*S*, 11'*R*, 10'*S*, 9'*S*, 11*R*, 10*S*, 9*S*, 15*S* absolute configuration (Figure S22).[11]

Compound **3** was obtained as a yellow amorphous solid and had the molecular formula $C_{22}H_{23}Br_2ClN_{10}O_3$, isomeric to compound **2**, deduced from its $[M+H]^+$ ion at *m/z* 669.0095 by HRESIMS analysis. Analysis of the NMR data revealed the same core skeleton of **2**, with the 4,5-dibromopyrrole carbonyl moiety attached at NH-7. Differences included a signal of a pyrrole N-H at δ_{NH} 11.91 (br s, H-1') and only two signals of the non-brominated pyrrole at δ_H 6.99 (t, *J*= 2.5 Hz, H-5') and 6.18 (t, *J*= 2.5 Hz, H-4'). Such differences suggested that compound **3** was a 4',5'-didebromo analogue of styloguanidine characterized by the reversal of the nitrogen of the pyrrole from position 1' to 3' when compared to the palau'amine alkaloids.[7] Such hypothesis was confirmed by the shielding of the signal H-15' at δ_H 5.47 (s) in **3**. ^{1}H and ^{13}C NMR data of **3** were consistent with data reported for carteramine A,[6] and tetrabromostyloguanidine (NMR data of **3** in Table S5).[13] The relative configuration of **3** was assumed as the same as compounds **2** and of palau'amine congeners considering similar ^{13}C NMR chemical shifts and NOESY correlations. To the best of our knowledge, the absolute configuration of styloguanidines and carteramines was not determined and, using a comparison between experimental and theoretical ECD spectra, we were able to assign the same absolute configurations as **2** (Figure S30).

The biosynthetic pathway of the PIA family has been a long-standing subject of debate.[14] We propose that futunamine (**1**) maybe be produced starting by a C-9/C-10' linkage between the oxidised clathrodin and oroidin (Scheme 1).[15, 16] A subsequent conjugated addition of N-12' onto the electrophilic enamine carbon C-10 would lead to the key pyrrolo[1,2-*c*]imidazole core of this new skeleton. The C-9/C-10' and C-10/N-12' linkages rule out other possible biosynthetic origins recently proposed for dimeric PIAs that start from sceptrin connected through C-9/C-9' and C-10/C-10'.[17] The linkages between the two 'oroidin-like' monomers in futunamine (**1**) is unique in the PIA family. This new skeleton reveals that the chemical diversity of PIAs is still expanding and should offer additional insights into their intriguing biosynthesis.

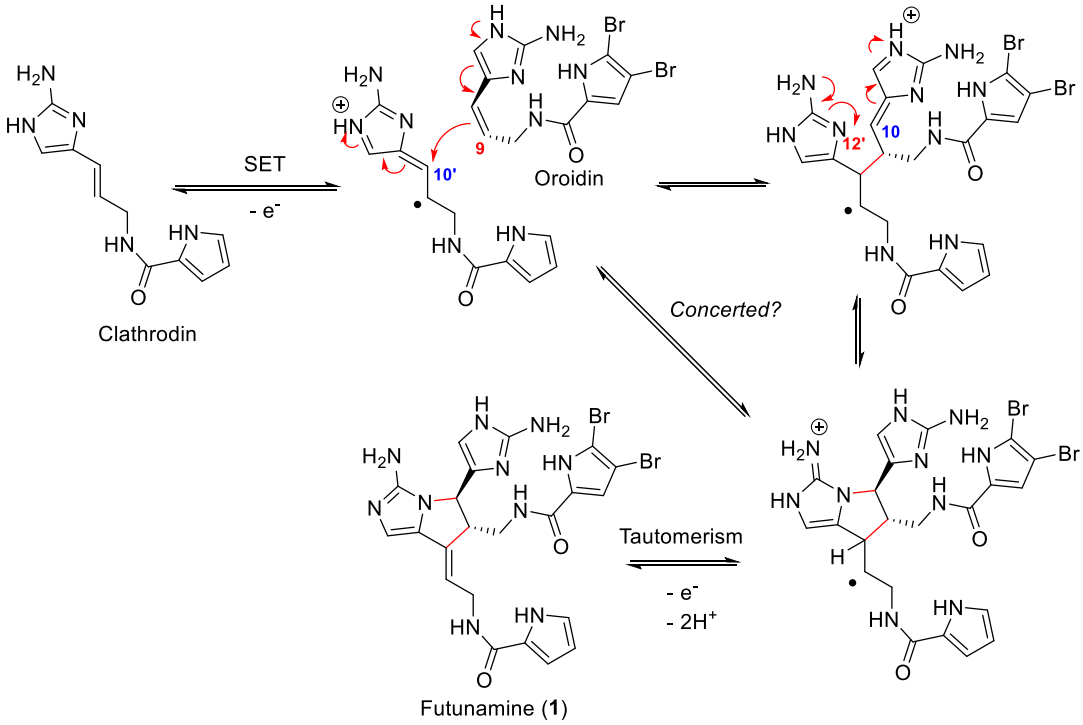

Scheme 1. Hypothesis for the methabolic pathway leading to futunamine (**1**)

The anti-inflammatory and neuroprotective activities of all isolated PIA metabolites were tested on two cellular models, human neuroblastoma SH-SY5Y and microglia BV2. No cytotoxic effects were observed at any concentration tested (Figure S1). Since ROS overproduction leads to

neuronal cell death,[18] the oxidant TBHP was used to increase ROS production, to induce neurotoxicity, and to evaluate the neuroprotective effect of the alkaloids isolated from *Stylissa* aff. *carteri*. Manzacidin A (**4**), hymenidin (**5**) and oroidin (**6**) showed neuroprotective effects at 0.001 μM (Figure S2). Cell death was decreased by **1** at 10 μM (Figure 3(a)). The next step was to check if compounds modulate the ROS production. Treatments of cells with TBHP increased cellular ROS production by 35%, and treatment with both TBHP and the positive control vitamin E reduced ROS to basal levels. Treatment of cells with TBHP, along with compounds **1** (Figure 3b) and **2** (Figure S3) reduced ROS production by 35%, in all tested concentrations. Additionally, compounds **4** and **5** decreased ROS production by more than 25 % up to 1 μM (Figure S3). Moreover, the biphasic activity showed by compounds **4** and **5** is common in antioxidant agents. As high levels of NO increase neuronal damage, the potential of these compounds to inhibit NO release was evaluated. LPS was employed to activate microglia BV2 cells stimulating inflammatory conditions. The presence of **2** and **5** (0.1 and 1 μM) significantly reduced NO release (Figure S4).

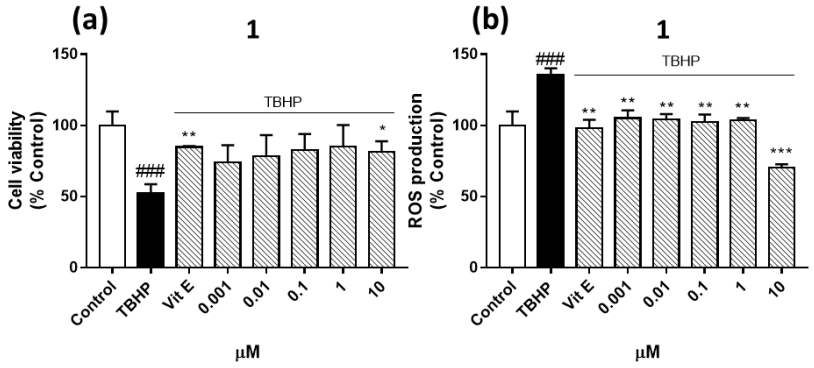

Figure 3. Effect of futunamine (**1**) on oxidative damage (a) and intracellular ROS production (b) in TBHP-stimulated neuroblastoma SH-SY5Y cell line. Cells were treated with compounds at different concentrations (0.001, 0.01, 0.1, 1 and 10 μM) in the presence of TBHP (65 μM) for 6 h.

Vitamin E (25 µM) was used as a positive control. Cell viability was measured by MTT assay (a). ROS levels were measured with DCFH-DA dye (b). Data are represented as percentage, being the result of the average of absorbance ± SEM of a minimum of N = 3 independent experiments performed by triplicate. Statistical analysis: ANOVA followed by post hoc Dunnet's t-test. Significant differences between cells treated with TBHP alone versus cells treated with compounds in presence of TBHP (*$p < 0.05$, **$p < 0.01$ and ***$p < 0.001$) or cells treated with TBHP versus control cells (###$p < 0.001$).

EXPERIMENTAL SECTION

General Experimental Procedures.

Optical rotation measurements were carried out at the Na D line (589.3 nm) with a 5 cm cell at 20 ºC on a UniPol L1000 polarimeter (Schmidt + Haensch, Berlin, Germany). UV and ECD data were obtained on a Chirascan V100 spectrophotometer (Applied Photophysics, Leatherhead, U.K.). NMR experiments were performed on a Varian Inova 500 MHz spectrometer with a 5 mm OneNMR probe (Varian, Palo Alto, CA, U.S.) and on a Agilent Premium Compact 600 MHz spectrometer with a 5 mm Cryoprobe (Agilent, California, U.S). Chemical shifts were referenced in ppm to the residual solvent signals (CD_3OD, at δ_H 3.31 and δ_C 49.00 ppm; DMSO-d_6, at δ_H 2.50 and δ_C 39.52 ppm). High-resolution mass spectra data were obtained with an Agilent 6540 q-Tof mass spectrometer UHPLC-DAD-HRMS (Agilent 6540, Santa Clara, CA, U.S). Purifications were performed using HPLC-UV equipped with a Jasco PU-2087 pump and UV-2075 detector (Tokyo, Japan).

Biological Material.

The biological material was collected around Wallis and Futuna Islands in December 2016 during the *Tara* pacific expedition and identified by Christine Morrow. Five specimens of *Stylissa*

aff. *carteri* were collected by scuba diving at depths between 6-15m at the collection sites (14º 21' 47'' S, 178º 02' 55'' W), (14º 17' 34'' S, 178º 04' 56'' W), (14º 19' 14'' S, 178º 03' 26'' W), (14º 18' 51'' S, 178º 07' 30'' W) and (14º 18' 50'' S, 178º 04' 41'' W). For taxonomic studies a fragment was fixed with EtOH and for chemical studies the rest of the samples were freeze dried and stored at -80 ºC. Voucher specimen MBNUIG853 nº161214Fu07-07 is stored at NUIG (National University of Ireland, Ireland). (See Supplementary information for more details).

Extraction and Isolation.

The freeze-dried specimens of the sponge *Stylissa* aff. *carteri* (92.7 g) were extracted with MeOH:CH_2Cl_2 (75:25, 3x500ml) by sonication. The dried extract (18.4 g) was sequentially fractionated by flash silica C-18 vacuum liquid chromatography in 8 fractions with solvents of decreasing polarity: H_2O, H_2O/MeOH (80:20), (60:40), (40:60) and (20:80), MeOH, MeOH/CH_2Cl_2 and CH_2Cl_2.

The H_2O/MeOH (40:60) fraction (1.2 g) was separated into 8 subfractions by repeated preparative RP-HPLC on a C-18 column (Waters Xselect, 5µm; 19x250 mm; flow rate 12.0 ml/min) using a gradient of solvents H_2O:CH_3CN/0.1% TFA (82:18, 4 min; ramp to 60:40 to 15 min; 60:40 for 5 min and back to 82:18 in 1 min). The subfraction 7 (R_t 14-16 min, 18.94 mg) was fractionated through semi-preparative RP-HPLC on a C18 column (Waters SymmetryPrep, 7 µm; 7.8 × 300 mm; flow rate: 2.3 ml/min) with H_2O:MeOH/0.1% TFA as mobile phase using an isocratic method (53:47, 25 min). This yielded compounds **1** (t_R 13 min, 2.1 mg, 2.3×10^{-3} % w/w), **2** (t_R 19 min, 3.4 mg, 3.7×10^{-3} % w/w), **3** (t_R 15 min, 1.4 mg, 1.5×10^{-3} % w/w), sceptrin (t_R 21 min, 1.0 mg) and **4** (t_R 17 min, 2.4 mg, 2.6×10^{-3} % w/w). The semi-preparative purification of subfraction 6 (t_R 13-14 min, 25.5 mg) using the same column and mobile phase as subfraction 7

and an isocratic method (65:35, 25 min), yielded compounds **5** (t_R 13 min, 4.0 mg, 4.3 × 10^{-3} % w/w) and **6** (t_R 19 min, 1.0 mg, 1.0 × 10^{-3} % w/w).

Futunamine (**1**): Yellow amorphous solid. $[\alpha]_D^{20}$ +42 (*c* 0.14, MeOH); UV (H_2O) λ_{max} (log ε) 244 (3.88), 277 (4.17) nm; ECD (*c* 1.18 × 10^{-4} M, H_2O) λ_{max} ($\Delta\varepsilon$) 235 (+0.42), 254 (−0.55), 274 (+1.12), 340 (+0.21) nm; (+)-HRESIMS *m/z* 617.0382 $[M + H]^+$ (calcd. for $C_{22}H_{23}{}^{79,79}Br_2N_{10}O_2^+$, 617.0367, Δ +2.4 ppm); for ^1H and ^{13}C NMR data, see Table 1.

Debromokonbu'acidin (**2**): Yellow amorphous solid. $[\alpha]_D^{20}$ −4.2 (*c* 0.33, MeOH); UV (H_2O) λ_{max} (log ε) 250 (3.76), 279 (4.12) nm; ECD (*c* 1.11 × 10^{-4} M, H_2O) λ_{max} ($\Delta\varepsilon$) 220 (−3.69), 248 (−0.85), 275 (+1.55) nm; (+)-HRESIMS *m/z* 669.0092 $[M + H]^+$ (calcd. for $C_{22}H_{23}{}^{79,79}Br_2ClN_{10}O_3$, 669.0083, Δ +1.4 ppm); for ^1H and ^{13}C NMR data, see Table S5.

Didebromocarteramine (**3**): Yellow amorphous solid. $[\alpha]_D^{20}$ +22 (*c* 0.11, MeOH); UV (H_2O) λ_{max} (log ε) 246 (3.64), 279 (4.06) nm; ECD (*c* 1.11 × 10^{-4} M, H_2O) λ_{max} ($\Delta\varepsilon$) 235 (+1.78), 274 (+1.82), 308 (−0.28) nm; (+)-HRESIMS *m/z* 669.0095 $[M+H]^+$ (calcd. for $C_{22}H_{23}{}^{79,79}Br_2{}^{35}ClN_{10}O_3$, 669.0083, Δ +1.8 ppm); for ^1H and ^{13}C NMR data, see Table S5.

Computational details

All DFT calculations were performed using Gaussian 16.[19] A conformational analysis of the core structure of **1** (Figure S6) was performed in Schrodinger Maestro Macromodel (ΔE threshold = 5.0 kcal/mol, forcefield = OPLS3). Following this a geometry optimization and a frequency check was conducted at the M062X/6-31g(d,p) level. Total nuclear spin-spin coupling J (Hz) was then predicted using the gauge-including atomic orbital (GIAO) method at MPW1PW91/6-311+G(2d,p) level. The coupling constants were then Boltzmann weighted to produce an overall estimate for each configuration. After the assignment of the relative configuration another conformational analysis of the full structure of **1** was performed in Schrodinger Maestro Macromodel (ΔE threshold = 3.0 kcal/mol, forcefield = OPLS3). Again a geometry optimization,

followed by a frequency check was conducted at the M062X/6-31g(d,p) level. The rotational strength was then calculated using TDDFT at the B3LYP/6.31g level for 50 excited states on all conformers. ECD spectra were obtained after Boltzmann averaging and UV correction using Specdis 1.7 (Figure S9).[20]

For compound **3** a conformational analysis was performed with the GMMX package (ΔE threshold=3.5 kcal/mol, forcefield=MMFF94). This was followed by a geometry optimization and frequency check conducted at the B3LYP/6-31g(d) level on the 5 major conformers. Rotational strength was then calculated using TDDFT at the B3LYP/6.31g level for 20 excited states. ECD spectra were obtained after Boltzmann averaging using GaussView 6.0.

Biological assays.

The purity of all tested compounds was assessed as >95% based on their ^{1}H NMR spectra. The 3-(4,5-dimethyl thiazol-2-yl)-2,5-diphenyl tetrazolium bromide (MTT) test was employed to analyzed cell viability and to perform the neuroprotection assay as described before.[21] The intracellular reactive oxygen species (ROS) levels were measured using 7′,2′-dichlorofluorescein diacetate (DCFH-DA), as previously described. [22] The nitric oxide (NO) concentration in the culture media was established using the Griess reagent kit, following the manufacturer's instructions. (See supporting information for more details)

ASSOCIATED CONTENT

Supplementary experimental section. Biological assays graphs. ^{1}H and ^{13}C NMR table and ECD spectra of compounds **2** and **3**. NMR and MS spectra of compounds **1**-**6** and sceptrin. *Tara* Pacific Consortium members acknowledgement.

AUTHOR INFORMATION

Corresponding Author

olivier.thomas@nuigalway.ie, +353-91493563; luis.botana@usc.es, + 34-982 822 233

ORCID:

Maria Miguel-Gordo: https://orcid.org/0000-0002-3252-9043

Sandra Gegunde: https://orcid.org/0000-0001-5576-7055

Grégory Genta-Jouve: http://orcid.org/0000-0002-9239-4371

Kevin Calabro: https://orcid.org/0000-0001-8962-4810

Laurence K. Jennings: https://orcid.org/0000-0002-1313-0360

Amparo Alfonso: https://orcid.org/0000-0003-1572-9016

Luis M. Botana: https://orcid.org/0000-0003-2153-6608

Olivier P. Thomas: http://orcid.org/0000-0002-5708-1409

Funding Sources

We are keen to thank the commitment of the people and the institutions mentioned in the SI for their financial and scientific support that made this singular expedition possible. *Tara* Pacific would not exist without the continuous support of the participating institutes. M.M.G. acknowledges James Hardiman Research Scholarship (NUI Galway) for supporting her Ph.D. The research leading to the results on bioassays has received funding from institutions cited in the SI.

ACKNOWLEDGMENTS

We are deeply grateful to the *Tara* Ocean Foundation teams and crew and the members of the *Tara* Pacific Consortium (See Supporting information) for their support during the

field trip to Futuna. Support and permission to undertake this study were provided by Atoloto Malau (Service de l'environnement, Wallis and Futuna). Roisin Doohan (NUIG) is acknowledged for recording some NMR experiments and Delphine Richard for her help in isolating the compounds. We acknowledge the Irish center for high-end computing (ICHEC) for their support and access to the computational resources for DFT calculations. We are grateful to Dr Christine Morrow for the sponge identification.

REFERENCES

1. Lindel, T., Chapter Three - Chemistry and Biology of the Pyrrole–Imidazole Alkaloids. In *The Alkaloids: Chemistry and Biology*, Knölker, H.-J., Ed. Academic Press 2017; Vol. 77, pp 117-219.
2. Al-Mourabit, A.; Zancanella, M. A.; Tilvi, S.; Romo, D., *Biosynthesis, asymmetric synthesis, and pharmacology, including cellular targets, of the pyrrole-2-aminoimidazole marine alkaloids*. *Nat. Prod. Rep.* **2011,** *28*, 1229-1260.
3. Planes, S.; Allemand, D.; Agostini, S.; Banaigs, B.; Boissin, E.; Boss, E.; Bourdin, G.; Bowler, C.; Douville, E.; Flores, J. M.; Forcioli, D.; Furla, P.; Galand, P. E.; Ghiglione, J.-F.; Gilson, E.; Lombard, F.; Moulin, C.; Pesant, S.; Poulain, J.; Reynaud, S.; Romac, S.; Sullivan, M. B.; Sunagawa, S.; Thomas, O. P.; Troublé, R.; de Vargas, C.; Vega Thurber, R.; Voolstra, C. R.; Wincker, P.; Zoccola, D.; the Tara Pacific, C., *The Tara Pacific expedition—A pan-ecosystemic approach of the "-omics" complexity of coral reef holobionts across the Pacific Ocean*. *PLoS Biol.* **2019,** *17*, e3000483.
4. Randazzo, A.; Dal Piaz, F.; Orru, S.; Debitus, C.; Roussakis, C.; Pucci, P.; Gomez-Paloma, L., *Axinellins A and B: New proline-containing antiproliferative cyclopeptides from the Vanuatu sponge Axinella carteri*. *Eur. J. Org. Chem.* **1998,** *1998*, 2659-2665.
5. Patel, K.; Laville, R.; Martin, M. T.; Tilvi, S.; Moriou, C.; Gallard, J. F.; Ermolenko, L.; Debitus, C.; Al-Mourabit, A., *Unprecedented stylissazoles A-C from Stylissa carteri: another dimension for marine pyrrole-2-aminoimidazole metabolite diversity*. *Angew. Chem. Int. Ed.* **2010,** *49*, 4775-4779.
6. Kobayashi, H.; Kitamura, K.; Nagai, K.; Nakao, Y.; Fusetani, N.; Van Soest, R. W. M.; Matsunaga, S., *Carteramine A, an inhibitor of neutrophil chemotaxis, from the marine sponge Stylissa carteri*. *Tetrahedron Lett.* **2007,** *48*, 2127-2129.
7. Hamed, A. N. E.; Kamel, M. S.; Hamed, A. N. E.; Proksch, P.; Schmitz, R.; Watjen, W.; Bergermann, A.; Watjen, W.; Totzke, F.; Kubbutat, M.; Muller, W. E. G.; Youssef, D. T. A.; Bishr, M. M.; Edrada-Ebel, R., *Bioactive pyrrole alkaloids isolated from the Red Sea: marine sponge Stylissa carteri*. *Z. Naturforsch., C: Biosci.* **2018,** *73*, 199-210.
8. Ma, Z.; Wang, X.; Wang, X.; Rodriguez, R. A.; Moore, C. E.; Gao, S.; Tan, X.; Ma, Y.; Rheingold, A. L.; Baran, P. S.; Chen, C., *Asymmetric syntheses of sceptrin and massadine and evidence for biosynthetic enantiodivergence*. *Science* **2014,** *346*, 219-224.
9. Haber, M.; Carbone, M.; Ilan, M.; Gavagnin, M., *Structure of debromo-carteramine A, a novel bromopyrrole alkaloid from the Mediterranean sponge Axinella verrucosa*. *ARKIVOC* **2010**, 233-239.
10. Garcia, E. E.; Benjamin, L. E.; Fryer, R. I., *Reinvestigation into Structure of Oroidin, a Bromopyrrole Derivative from Marine Sponge*. *J. Chem. Soc. D* **1973**, 78-79.
11. Kobayashi, J.; Suzuki, M.; Tsuda, M., *Konbu'acidin A, a new bromopyrrole alkaloid with cdk4 inhibitory activity from Hymeniacidon sponge*. *Tetrahedron* **1997,** *53*, 15681-15684.
12. Lindel, T.; Jacquot, D. E. N.; Zöllinger, M.; Kinnel, R. B.; McHugh, S.; Köck, M., *Study on the absolute configuration of (−)-palau'amine*. *Tetrahedron Lett.* **2010,** *51*, 6353-6355.
13. Grube, A.; Kock, M., *Structural assignment of tetrabromostyloguanidine: does the relative configuration of the palau'amines need revision? Angew. Chem. Int. Ed.* **2007,** *46*, 2320-2324.

14. Al Mourabit, A.; Potier, P., *Sponge's Molecular Diversity Through the Ambivalent Reactivity of 2-Aminoimidazole: A Universal Chemical Pathway to the Oroidin-Based Pyrrole-Imidazole Alkaloids and Their Palau'amine Congeners*. *Eur. J. Org. Chem.* **2001,** *2001*, 237-243.
15. Genta-Jouve, G.; Cachet, N.; Holderith, S.; Oberhansli, F.; Teyssie, J. L.; Jeffree, R.; Al Mourabit, A.; Thomas, O. P., *New insight into marine alkaloid metabolic pathways: revisiting oroidin biosynthesis*. *ChemBioChem* **2011,** *12*, 2298-2301.
16. Stout, E. P.; Wang, Y.-G.; Romo, D.; Molinski, T. F., *Pyrrole Aminoimidazole Alkaloid Metabiosynthesis with Marine Sponges Agelas conifera and Stylissa caribica*. *Angew. Chem. Int. Ed.* **2012,** *51*, 4877-4881.
17. O'Malley, D. P.; Li, K.; Maue, M.; Zografos, A. L.; Baran, P. S., *Total synthesis of dimeric pyrrole-imidazole alkaloids: sceptrin, ageliferin, nagelamide e, oxysceptrin, nakamuric acid, and the axinellamine carbon skeleton*. *J. Am. Chem. Soc.* **2007,** *129*, 4762-4775.
18. Leirós, M.; Alonso, E.; Rateb, M. E.; Houssen, W. E.; Ebel, R.; Jaspars, M.; Alfonso, A.; Botana, L. M., *Gracilins: Spongionella-derived promising compounds for Alzheimer disease*. *Neuropharmacology* **2015,** *93*, 285-293.
19. Frisch, M. J.; Trucks, G. W.; Schlegel, H. B.; Scuseria, G. E.; Robb, M. A.; Cheeseman, J. R.; Scalmani, G.; Barone, V.; Petersson, G. A.; Nakatsuji, H.; Li, X.; Caricato, M.; Marenich, A. V.; Bloino, J.; Janesko, B. G.; Gomperts, R.; Mennucci, B.; Hratchian, H. P.; Ortiz, J. V.; Izmaylov, A. F.; Sonnenberg, J. L.; Williams; Ding, F.; Lipparini, F.; Egidi, F.; Goings, J.; Peng, B.; Petrone, A.; Henderson, T.; Ranasinghe, D.; Zakrzewski, V. G.; Gao, J.; Rega, N.; Zheng, G.; Liang, W.; Hada, M.; Ehara, M.; Toyota, K.; Fukuda, R.; Hasegawa, J.; Ishida, M.; Nakajima, T.; Honda, Y.; Kitao, O.; Nakai, H.; Vreven, T.; Throssell, K.; Montgomery Jr., J. A.; Peralta, J. E.; Ogliaro, F.; Bearpark, M. J.; Heyd, J. J.; Brothers, E. N.; Kudin, K. N.; Staroverov, V. N.; Keith, T. A.; Kobayashi, R.; Normand, J.; Raghavachari, K.; Rendell, A. P.; Burant, J. C.; Iyengar, S. S.; Tomasi, J.; Cossi, M.; Millam, J. M.; Klene, M.; Adamo, C.; Cammi, R.; Ochterski, J. W.; Martin, R. L.; Morokuma, K.; Farkas, O.; Foresman, J. B.; Fox, D. J. *Gaussian 16 Rev. C.01*, Wallingford, CT, 2016.
20. Bruhn, T.; Schaumloffel, A.; Hemberger, Y.; Bringmann, G., *SpecDis: quantifying the comparison of calculated and experimental electronic circular dichroism spectra*. *Chirality* **2013,** *25*, 243-249.
21. Burton, J. D., The MTT Assay to Evaluate Chemosensitivity. In *Chemosensitivity: Volume 1 In Vitro Assays*, Blumenthal, R. D., Ed. Humana Press: Totowa, NJ, 2005; pp 69-78.
22. Wu, Y.; Shang, Y.; Sun, S.; Liu, R., *Antioxidant effect of erythropoietin on 1-methyl-4-phenylpyridinium-induced neurotoxicity in PC12 cells*. *Eur. J. Pharmacol.* **2007,** *564*, 47-56.

TOC